

**S. Paeme\*, K. Moorhead\*, J.G. Chase\*\*, CE. Hann\*\*, B. Lambermont\*, P. Kolh\*,  
M. Moonen\*, P. Lancellotti\*, P.C. Dauby\*, T. Desai\***

**\*\* Department of Mechanical Engineering, University of Canterbury, Christchurch, New Zealand**

**Keywords:** cardiovascular system model, valve dynamics, mitral valve, mitral insufficiency, cardiac cycle

This work was supported by the F.R.I.A. (Belgium), the University of Canterbury and the French Community of Belgium (Actions de Recherches Concertées Académie Wallonie-Europe)

The cardiac chambers are modeled using pressure-volume (PV) relationships. The upper and lower limits of the cardiac cycle (Figure 2), respectively the end systolic pressure-volume relationship (ESPVR) and the end diastolic pressure-volume relationship (EDPVR) are defined:

$$ESPVR : P_{ES}(V) = E_{ES}(V - V_d) \quad (1)$$

$$EDPVR : P_{ED}(V) = A(e^{\lambda(V-V_0)} - 1) \quad (2)$$

where  $P_{ES}$  is the end-systolic pressure,  $E_{ES}$  the end-systolic elastance,  $V$  the volume,  $V_d$  the volume at zero pressure,  $P_{ED}$  the end-diastolic pressure and  $A, \lambda, V_0$  are three parameters of the nonlinear relationship.

To account for myocardial activation, a time-varying elastance driving function is used over a single heart beat and is defined:

$$e(t) = e^{-80(t-0.27)^2} \quad (3)$$

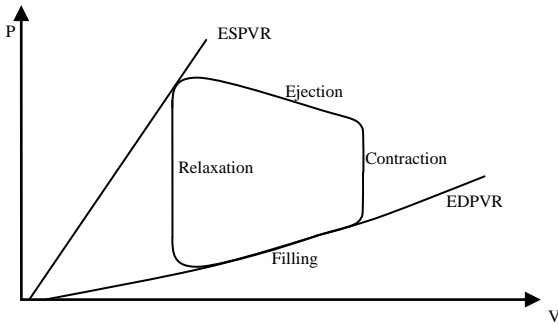


Fig. 2. Pressure-volume diagram

There are three differential equations describing the rate of change of the cardiac chamber volume and the inflow ( $Q_{in}$ ) and outflow ( $Q_{out}$ ) for each ventricle:

$$\frac{dV}{dt} = Q_{in} - Q_{out} \quad (4)$$

$$\frac{dQ_{in}}{dt} = \frac{P_{up} - P - Q_{in}R_{in}}{L_{in}} \quad (5)$$

$$\frac{dQ_{out}}{dt} = \frac{P - P_{down} - Q_{out}R_{out}}{L_{out}} \quad (6)$$

where  $P_{up}$ ,  $P_{down}$  and  $P$  are the upstream, the downstream and the chamber pressures,  $L_{out}$  and  $L_{in}$  respectively the outer and inner inductors, and  $R_{out}$  and  $R_{in}$  the outer and inner resistances. These equations are valid for the six chambers of our model.

### Ventricular interaction and valve dynamics

Both the septum and the pericardium play major roles in ventricular interaction as they link the two chambers directly.

To define the septum volume  $V_{spt}$  we introduce the free wall volumes  $V_{lvf}$  and  $V_{rvf}$  which are not exactly physical volumes. They are defined in Figure 3.

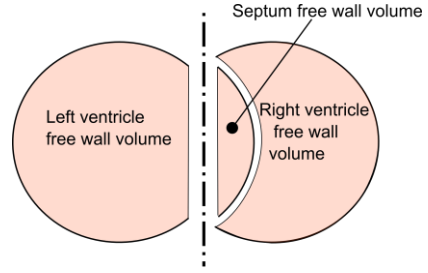


Fig. 3. Free wall volumes definitions in the heart

At each time step,  $V_{spt}$  is obtained from the following nonlinear equation (Smith et al., 2004):

$$\begin{aligned} e(t)E_{es,spt}(V_{spt} - V_{d,spt}) + (1 - e(t))P_{0,spt}(e^{\lambda_{spt}(V_{spt} - V_{0,spt})} - 1) \\ = e(t)E_{es,lvf}(V_{lv} - V_{spt}) + (1 - e(t))P_{0,lvf}(e^{\lambda_{lvf}(V_{lv} - V_{spt})} - 1) \\ - e(t)E_{es,rvf}(V_{rv} + V_{spt}) - (1 - e(t))P_{0,rvf}(e^{\lambda_{rvf}(V_{rv} + V_{spt})} - 1) \end{aligned} \quad (7)$$

where  $E_{es,spt}$ ,  $E_{es,lvf}$ ,  $E_{es,rvf}$ ,  $V_{0,spt}$ ,  $V_{d,spt}$ ,  $\lambda_{rvf}$  and  $\lambda_{lvf}$  are parameters defined in (Smith et al., 2004).

Finally, the model used in this paper assumes that the 4 cardiac valves only exist in two different states: open or closed (Smith et al., 2004). Thus, a special procedure is used (Hann et al., 2005) that automatically accounts for the valves opening and closing, instead of using an event solver to detect when the valve should open or close. This procedure is based on the Heaviside formulation in Equation and minimises computation and computational instability (Hann et al., 2005).

$$H(x) = \begin{cases} 0 & \text{if } x \leq 0 \\ 1 & \text{if } x > 0 \end{cases} \quad (8)$$

For each valve, the argument of the Heaviside function is chosen to fulfil the law: “open on pressure, close on flow” (Smith et al., 2004, Hann et al., 2005).

### 2.2 The mitral valve model

The main drawback of the Heaviside formulation is that it does not take into account physiological time scale of the valve aperture (Saito et al., 2006). Therefore, the initial model is not able to fully capture valve dysfunctions. Given the common occurrence of valve dysfunction, it has important clinical implications.

The normal motion of the mitral valve during a cardiac cycle has been analyzed by Saito et al. (Saito et al., 2006). The qualitative normal mitral aperture evolution during the

diastole is given in Figure 4. It describes the two peaks E-wave and A-wave corresponding respectively to the passive filling of the ventricle and the active one, due to the atrial contraction.

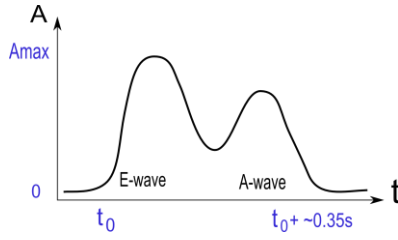


Fig. 4. Effective mitral aperture evolution during the filling phase (diastole), shown schematically

A first attempt to describe the progressive aperture of the mitral valve was made by Szabó and co-workers (Szabó et al., 2004) but their model is only valid during the early ventricular filling phase. We will first describe this model and then explain how we extend it to the complete cardiac cycle.

The model begins at the time when pressures are equal in the atrium and the ventricle. It thus begins from the instant of mitral valve opening. The model then describes flow and pressures during ventricular filling up to the point of atrial systole. This model is then valid until the end of the early diastole also denoted as E-wave. The interval of validity of this model, the early diastolic ventricular filling phase, is shown in Figure 5.

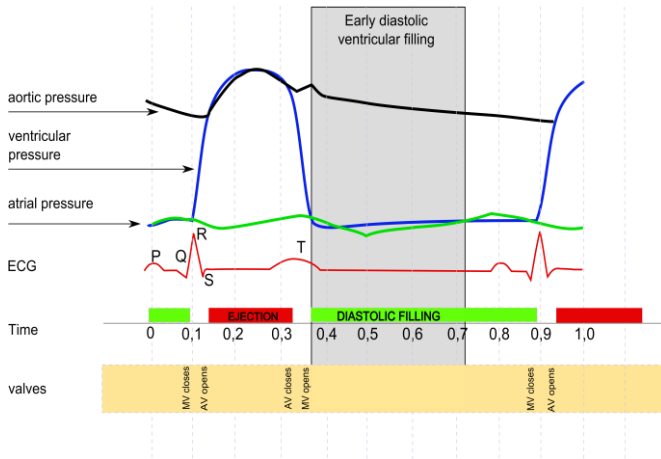


Fig. 5 A typical pressure waveform in the left atrium, left ventricle and aorta, the electrocardiogram evolution and the corresponding cardiac events. The section marked shows the period designated as “Early diastolic filling”.

The mitral apparatus is modelled as a cylinder of a cross-sectional area  $A$  and length  $l$  constant (Thomas and Weyman, 1989, Waite et al., 2000) (Figure 6). The concept of mitral valve impedance is derived from these two geometric parameters and other physiological parameters such as blood density and velocity (Waite and Fine, 2007).

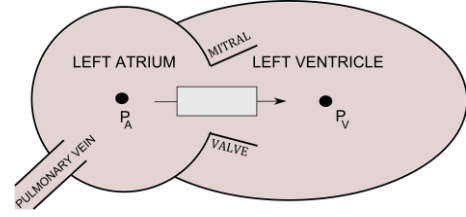


Fig. 6 Schematic of the left heart used to develop a mathematical model of flow through the mitral valve.

A system of three ordinary differential equations describes the system (Equations 9-11).

$$\frac{dq}{dt} = \frac{(P_A - P_V - R_V q - \text{sign}(q) R_C q^2)}{L} + V \frac{dA}{dt} \quad (9)$$

$$\frac{dP_A}{dt} = \frac{-q}{C_A} \quad (10)$$

$$\frac{dP_V}{dt} = \frac{q}{C_V} - \text{active relaxation term} \quad (11)$$

Where the active relaxation term captures the exponential decrease of the pressure independently of the changes of volume of the ventricle (Szabó et al., 2004).

This model uses the following variables and parameters:

$P_A$ = left atrial pressure	$P_V$ = left ventricular pressure
$q$ = instantaneous flow rate through the mitral valve	$R_V$ = viscous resistance
$R_C$ = convective resistance	$L$ = inertance term
$C_A$ = atrial compliance	$C_V$ = ventricular compliance
$A$ = mitral valve effective area	$V$ = average velocity of blood through the mitral valve

Using a systems approach, the mitral valve aperture is viewed abstractly as a mechanical system whose behaviour is governed by intrinsic dynamics and forces acting on it.

The intrinsic dynamics of the valve aperture are modelled by a second-order linear differential equation taking into account the mass of the valve cusps, the elasticity of the tissue and the damping experienced by the valve cusps, while minimising valve model complexity:

$$\frac{1}{\omega^2} \ddot{A} + \frac{2D}{\omega} \dot{A} + A = F(t) \quad (12)$$

Where  $D$  is the damping coefficient and describes the amount of damping the valve cusps experience,  $\omega$  is the natural frequency of the valve and  $F(t)$  models the forces acting on the valve.

This term is derived by considering Bernoulli's equation for unsteady, inviscid flow along a streamline. The equation states that on any point, the total pressure is composed of three components: static pressure, dynamic pressure and acceleration-induced pressure. These three components of the

fluid pressure inside the mitral valve apparatus lead to a force acting on the valve cusps.

$$F(t) = (A_{\max} - A) \left[ K_s (P_A - P_v) + K_d \cdot \text{sign}(v) v^2 + K_a \frac{dv}{dt} \right] \quad (13)$$

The force term contains the remaining 4 parameters  $A_{\max}$ ,  $K_s$ ,  $K_d$  et  $K_a$ , as defined in (Szabó et al., 2004).

### 2.3 Coupling both models

The model described in the previous section is only valid during a small part of the cardiac cycle (the E-wave). To couple it with the closed-loop CVS model, we need to have a valve model valid over a complete cardiac cycle.

However, the CVS model does not include a chamber for the left atrium so it does not capture strictly the atrial systole also referred to as the A-wave. In this research we propose a simplified approach to account for both the E-wave and the A-wave as illustrated in Figure 8.

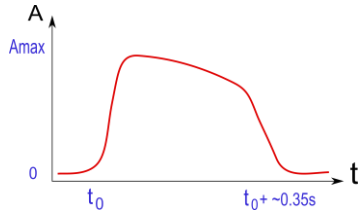


Fig. 7. Simplified mitral aperture evolution, shown schematically

This modified model of the variable mitral aperture is then introduced into the closed loop model of the CVS. To achieve this correction, the system of ordinary differential equations was modified. The Heaviside functions related to the mitral valve were deleted and replaced as defined hereafter.

Based on the expression of the resistance in a cylindrical flow, the mitral resistance is modified to be a function of the mitral aperture:

$$R_{mt} = \frac{8\pi\mu l}{A(t)^2} \quad (14)$$

In the same way, we adapt the expression of the inertance:

$$L_{mt} = \frac{\rho l}{A(t)} \quad (15)$$

The variation of the mitral flow  $q_{mt}$  is also updated to take into account the variation of the mitral aperture:

$$\dot{q}_{mt} = \frac{P_{pu} - P_{lv}}{L_{mt}} - q_{mt} \frac{R_{mt}}{L_{mt}} + \frac{q_{mt}}{A} \dot{A} \quad (16)$$

Thus this approach introduces two new state variables  $A$  and  $\dot{A}$  and consequently two new ordinary differential equations.

In summary, the new system of ordinary differential equations can be written:

$$\begin{aligned} \dot{V}_{pu} &= H(Q_{pul})Q_{pul} - q_{mt} \\ \dot{q}_{mt} &= \frac{P_{pu} - P_{lv}}{L_{mt}} - q_{mt} \frac{R_{mt}}{L_{mt}} + \frac{q_{mt}}{A} \dot{A} \\ \dot{V}_{lv} &= q_{mt} - H(q_{av})q_{av} \\ \dot{q}_{av} &= H(H(P_{lv} - P_{ao}) + H(q_{av}) - 0.5) \times \dots \\ &\quad \frac{P_{lv} - P_{ao} - q_{av}R_{av}}{L_{av}} \\ \dot{V}_{ao} &= H(q_{av})q_{av} - H(Q_{sys})Q_{sys} \\ \dot{V}_{vc} &= H(Q_{sys})Q_{sys} - H(q_{tc})q_{tc} \\ \dot{q}_{tc} &= H(H(P_{vc} - P_{rv}) + H(q_{tc}) - 0.5) \times \dots \\ &\quad \frac{P_{vc} - P_{rv} - q_{tc}R_{tc}}{L_{tc}} \\ \dot{V}_{vc} &= H(q_{tc})q_{tc} - H(q_{pv})q_{pv} \\ \dot{q}_{pv} &= H(H(P_{rv} - P_{pa}) + H(q_{pv}) - 0.5) \times \dots \\ &\quad \frac{P_{rv} - P_{pa} - q_{pv}R_{pv}}{L_{pv}} \\ \dot{V}_{rv} &= H(q_{pv})q_{pv} - H(Q_{pul})Q_{pul} \\ \dot{A} &= H(H(\dot{A}) + H(A) - 0.5)\dot{A} \\ \ddot{A} &= H(H(P_{pu} - P_{lv}) + H(A) - 0.5) \times \left\{ \dots \right. \\ &\quad (A_{\max} - A)(P_{pu} - P_{lv})c_1\omega^2 + \dots \\ &\quad (A_{\max} - A)(P_{pu} - P_{lv})c_2 \operatorname{sgn}\left(\frac{q_{mt}}{A}\right) \frac{q_{mt}}{A} \omega^2 - \dots \\ &\quad ((A_{\max} - A)c_3\omega^2) \times \dots \\ &\quad \left[ \frac{1}{A} \left( \frac{P_{pu} - P_{lv}}{L_{mt}} - q_{mt} \frac{R_{mt}}{L_{mt}} + \frac{q_{mt}}{A} \dot{A} \right) - \dots \right. \\ &\quad \left. \frac{1}{A^2} q_{mt} \dot{A} \right] + \dots \\ &\quad \left. Ac_4\omega^2 - \frac{2D}{\omega} \dot{A} c_5\omega^2 \right\} \end{aligned} \quad (17)$$

We simulate the model with Matlab (The MathWorks, USA) and solve the system of ordinary differential equations with the ode45 routine.

### 3. RESULTS

The models of Sections 2.1 and 2.3 are simulated for a healthy human (Smith et al., 2004). Figure 9 shows the left and right PV-loops using the original model of Section 2.1. Figure 10 shows the same simulation with a healthy mitral valve but for the model of Section 2.3.

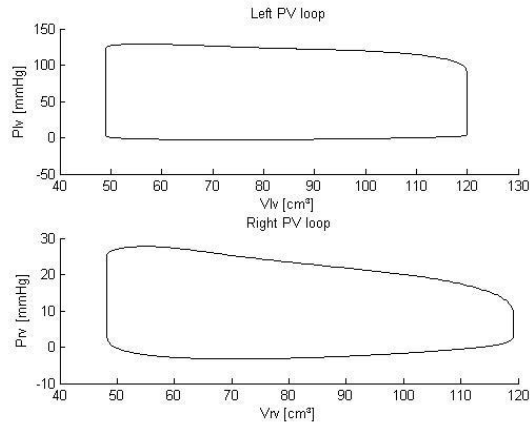


Fig. 8. Pressure-Volume loops for the model introduced in the Sec. 2.1 for the left and right ventricles.

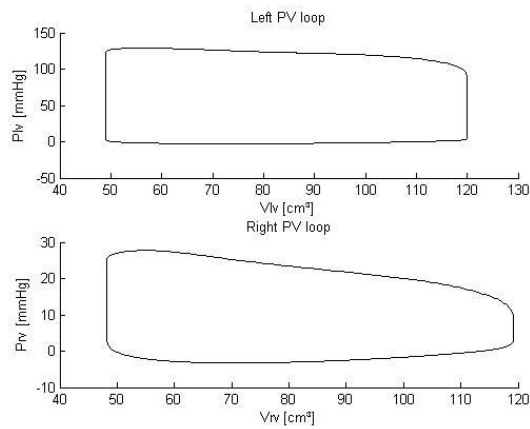


Fig. 9. Pressure-Volume loop for the model introduced in the Sec. 2.3 for the left and right ventricles.

### 3.1 Comparison of the results

Comparing the simulations with the initial CVS model and the Heaviside valve law, with the new model including variable mitral valve aperture provides initial model validation. Hemodynamic variables trends in both models show very good correlation and the new model accurately describes the opening and closing of the valve as expected physiologically.

### 3.2 Mitral valve dysfunction

The new model is now evaluated for a common pathological situation, namely the mitral valve insufficiency. This pathology consists of a defect in the mitral valve structure and/or dynamics leading to mitral regurgitation (Lancellotti, 2004-2005, Raff et al., 2000), as shown in Figure 11.

Figure 12 shows schematically a typical pressure-volume loop for such a valvular dysfunction, as observed clinically (Raff et al., 2000).

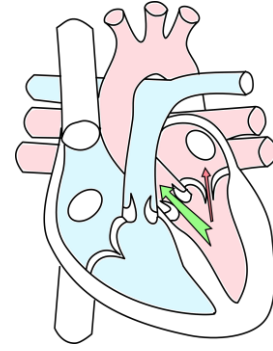


Fig. 10. Mitral regurgitation. The green arrow characterises the correct ejection from the ventricle to the aorta. The red arrow characterises the mitral regurgitation from the ventricle to the atrium during systole.

To model this situation, the parameters of the mitral valve model are modified close with some of the hemodynamic variables to take into account the cardiac adaptation to the pathology. Despite the large number of parameters realistic mitral valve regurgitation was simulated and resulted in and found pressure-volume loops in figure 13 comparable to those observed clinically.

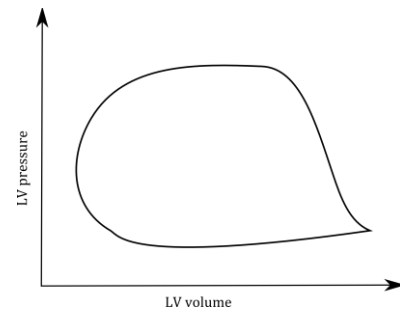


Fig. 11. Pressure-volume loop for a left ventricle with a mitral insufficiency, shown schematically.

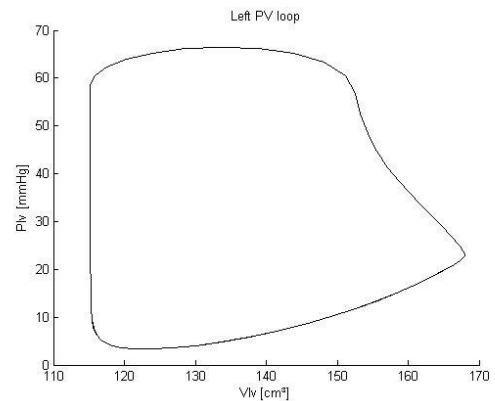


Fig. 12. Computed pressure-volume loop for the left ventricle

Hence, mitral valve regurgitation was simulated. The results very close in shape and magnitude to clinical results further validating the model.

#### 4. CONCLUSIONS

This work describes a new closed-loop model of the cardiovascular system that accounts for progressive mitral valve aperture. Simulations show good correlation with physiologically expected results for healthy or diseased valves. The large number of valve model parameters indicates a need for emerging, lighter and minimal mitral valve models that are readily identifiable to achieve full benefit in real-time use. These results suggest a further use of this model to track, diagnose and control valves pathologies.

#### 5. REFERENCES

- Burkhoff, D., Alexander, J. & Schipke, J. 1988. Assessment of Windkessel as a Model of Aortic Input Impedance. *American Journal of Physiology*, 255, H742-H753.
- Desaive, T., Ghuysen, A., Lambermont, B., Kolh, P., Dauby, P. C., Starfinger, C., Hann, C. E., Chase, J. & Shaw, G. M. 2007. Study of ventricular interaction during pulmonary embolism using clinical identification in a minimum cardiovascular system model. *Conf Proc IEEE Eng Med Biol Soc*, 2007, 2976-9.
- Desaive, T., Lambermont, B., Ghuysen, A., Kolh, P., Dauby, P. C., Starfinger, C., Hann, C. E., Chase, J. G. & Shaw, G. M. 2008. Cardiovascular Modelling and Identification in Septic Shock - Experimental validation. *Proceedings of the 17th IFAC World Congress July 6-11, 2008, Seoul, Korea*.
- Franck, C. F. & Waite, L. 2002. Mathematical model of a variable aperture mitral valve. *Biomedical Sciences Instrumentation*, 38, 327-31.
- Hann, C. E., Chase, J. G. & Shaw, G. M. 2005. Efficient implementation of non-linear valve law and ventricular interaction dynamics in the minimal cardiac model. *Computer Methods and Programs in Biomedicine*, 80, 65-74.
- Hunter, P. J., Nielsen, P. M. F., Smaill, B. H., Legrice, I. J. & Hunter, I. W. 1992. An Anatomical Heart Model with Applications to Myocardial Activation and Ventricular Mechanics. *Critical Reviews in Biomedical Engineering*, 20, 403-&.
- Kerckhoffs, R. C. P., Neal, M. L., Gu, Q., Bassingthwaite, J. B., Omens, J. H. & McCulloch, A. D. 2007. Coupling of a 3D finite element model of cardiac ventricular mechanics to lumped systems models of the systemic and pulmonary circulation. *Annals of Biomedical Engineering*, 35, 1-18.
- Lancellotti, P. 2004-2005. *L'insuffisance mitrale dynamique : le rôle de l'échocardiographie d'effort*. PhD, Université de Liège.
- Olsen, J. B., Clark, J. W., Khoury, D., Ghorbel, F. & Bidani, A. 2000. A closed-loop model of the canine cardiovascular system that includes ventricular interaction. *Computers and Biomedical Research*, 33, 260-95.
- Raff, U., Culclasure, T. F., Clark, C., Overturf, L. & Groves, B. M. 2000. Computerized left ventricular pressure-volume relationships (pv-loops) using disposable angiographic tip transducer pigtail catheters. *International Journal of Cardiac Imaging*.
- Saito, S., Araki, Y., Usui, A., Akita, T., Oshima, H., Yokote, J. & Ueda, Y. 2006. Mitral valve motion assessed by high-speed video camera in isolated swine heart. *Eur J Cardiothorac Surg*, 30, 584-91.
- Shim, E. B., Jun, H. M., Leem, C. H., Matusuoka, S. & Noma, A. 2008. A new integrated method for analyzing heart mechanics using a cell-hemodynamics-autonomic nerve control coupled model of the cardiovascular system. *Progress in Biophysics and Molecular Biology*, 96, 44-59.
- Smith, B. W., Chase, J. G., Nokes, R. I., Shaw, G. M. & Wake, G. 2004. Minimal haemodynamic system model including ventricular interaction and valve dynamics. *Medical Engineering and Physics*, 26, 131-9.
- Smith, B. W., Geoffrey Chase, J., Shaw, G. M. & Nokes, R. I. 2005. Experimentally verified minimal cardiovascular system model for rapid diagnostic assistance. *Control Engineering Practice*, 13, 1183-1193.
- Starfinger, C., Chase, J. G., Hann, C. E., Shaw, G. M., Lambermont, B., Ghuysen, A., Kolh, P., Dauby, P. C. & Desaive, T. 2008a. Model-based identification and diagnosis of a porcine model of induced endotoxic shock with hemofiltration. *Mathematical Biosciences*, 216, 132-9.
- Starfinger, C., Chase, J. G., Hann, C. E., Shaw, G. M., Lambert, P., Smith, B. W., Sloth, E., Larsson, A., Andreassen, S. & Rees, S. 2008b. Model-based identification of PEEP titrations during different volemic levels. *Computer Methods and Programs in Biomedicine*, 91, 135-144.
- Starfinger, C., Hann, C. E., Chase, J. G., Desaive, T., Ghuysen, A. & Shaw, G. M. 2007. Model-based cardiac diagnosis of pulmonary embolism. *Computer Methods and Programs in Biomedicine*, 87, 46-60.
- Szabó, G., Soans, D., Graf, A., J. Beller, C., Waite, L. & Hagl, S. 2004. A new computer model of mitral valve hemodynamics during ventricular filling. *European Journal of Cardio-Thoracic Surgery*, 26, 239-247.
- Thomas, J. D. & Weyman, A. E. 1989. Fluid dynamics model of mitral valve flow: description with in vitro validation. *Journal of the American College of Cardiology*, 13, 221-33.
- Waite, L. & Fine, J. M. 2007. *Applied biofluid mechanics*, New York, McGraw-Hill.
- Waite, L., Schulz, S., Szabo, G. & Vahl, C. F. 2000. A lumped parameter model of left ventricular filling-pressure waveforms. *Biomedical Sciences Instrumentation*, 36, 75-80.